PHYSICAL REVIEW C VOLUME 30, NUMBER 2 AUGUST 1984

# Nonstatic, self-consistent $\pi$N $t$ matrix in nuclear matter

J. W. Van Orden
*Department of Physics and Astronomy, University of Maryland, College Park, Maryland 20742*
(Received 7 September 1983)

In a recent paper, a calculation of the self-consistent $\pi$N $t$ matrix in nuclear matter was presented. In this calculation the driving term of the self-consistent equation was chosen to be a static approximation to the free $\pi$N $t$ matrix. In the present work, the earlier calculation is extended by using a nonstatic, fully-off-shell free $\pi$N $t$ matrix as a starting point. Right-hand pole and cut contributions to the $P$-wave $\pi$N amplitudes are derived using a Low expansion and include effects due to recoil of the interacting $\pi$N system as well as the transformation from the $\pi$N c.m. frame to the nuclear rest frame. The self-consistent $t$-matrix equation is rewritten as two integral equations which modify the pole and cut contributions to the $t$ matrix separately. The self-consistent $\pi$N $t$ matrix is calculated in nuclear matter and a nonlocal optical potential is constructed from it. The resonant contribution to the optical potential is found to be broadened by 20% to 50% depending on pion momentum and is shifted upward in energy by approximately 10 MeV in comparison to the first-order optical potential. Modifications to the nucleon pole contribution are found to be negligible.

## I. INTRODUCTION

In a recent paper,[1] a new organization of pion-nucleus scattering was presented. This organization is based on a Goldstone-diagrammatical treatment of the many-body problem and is centered around a self-consistent, effective pion-nucleon $t$ matrix in the nuclear medium.

This effective $t$ matrix is found by solving an integral equation which serves to replace the free pion propagator in elastic ($\pi$N) intermediate states of the $\pi$N $t$ matrix by a pion propagator distorted by the optical potential which describes elastic scattering of the pion from the residual nuclear system. The effective $t$ matrix is self-consistent in the sense that the optical potential, which dresses pion propagation in this integral equation for the effective $t$ matrix, is calculated using the same effective $t$ matrix. By allowing the intermediate state pion to interact with the residual nuclear system, channels associated with the many-body degrees of freedom of the nuclear system are introduced into intermediate states of the effective $t$ matrix. The effective $t$ matrix therefore reflects the possibility of flux being lost to absorption or knockout channels involving many nucleons. The self-consistent $t$ matrix has been calculated[2-6] or estimated[7] within a variety of models.

By using the Goldstone method, the new organization of $\pi$-nucleus scattering described in Ref. 1 can extend the concept of the self-consistent $t$ matrix to include all possible contributions to the $\pi$-nuclear optical potential. For example, modifications to the optical potential arising from scattering from correlated nucleon pairs may be included dynamically by adding diagrams involving the Brueckner $g$ matrix. Antisymmetry effects can be included by including diagrams involving nucleon exchange. Because the Goldstone method is based on field theory, it is also possible to consistently include contributions arising from the crossing symmetry of the basic free $\pi$N $t$ matrix and from nonsequential scattering effects where two scattering events overlap in time.

In addition to the description of the organization of $\pi$-nucleus scattering, Ref. 1 also included a simple model calculation of the self-consistent $\pi$N $t$ matrix in nuclear matter. In this calculation, the $P$-wave, right-hand cut and pole contributions to the free $\pi$N $t$ matrix were used as driving terms in the self-consistent $t$-matrix equation. For simplicity, effects associated with two-nucleon correlations, antisymmetry, and the crossed $\pi$N amplitudes were neglected. These effects have been examined in Ref. 8 in connection with a calculation of pion double scattering contributions to the pion-nucleus optical potential. Although nucleons were allowed to recoil freely above the Fermi sea between scattering in the calculation of Ref. 1, the $\pi$N $t$ matrices were static in that the interacting $\pi$N pair represented by the $t$ matrix was not allowed to recoil or propagate. The choice of the static $t$ matrix was made only to simplify the calculation which was intended only to study the qualitative effects of self-consistency. The self-consistent $t$ matrix was used to obtain a $\pi$-nuclear optical potential. Comparison of this self-consistent optical potential with the first order optical potential calculated with the free $\pi$N $t$ matrix showed several differences. The resonant contribution is broadened and shifted to a slightly higher energy as a result of multinucleon excitations in intermediate states of the effective $t$ matrix. This broadening is therefore dynamical in origin. The existence of intermediate states where the pion is absorbed on two or more nucleons increases the magnitude of the imaginary part of the optical potential at and below threshold. In solving for the self-consistent $t$ matrix, an effective $t$ matrix was calculated where intermediate state pion propagation was dressed by the optical potential derived from the free $t$ matrix rather than the self-consistent $t$ matrix. This effective $t$ matrix differed by only a small amount from the self-consistent $t$ matrix. Physically, this suggests that intermediate states involving two-nucleon excitations provide the dominant medium modifications to the $\pi$N $t$ matrix.

Although the simplicity of the static $\pi$N $t$ matrix is useful in performing simple model calculations where only qualitative features are to be studied, the static approximation does some violence to the physics of the $\pi$N interaction. This approximation neglects the transformation from the $\pi$N center-of-mass frame (where the partial wave decomposition of the $t$ matrix is defined) to the nuclear rest frame (where the nucleon wave functions are defined). This transformation modifies the scattering angle which appears in angular momentum projectors in the $t$ matrix and introduces a nonlocality in the $t$ matrix resulting from the recoil of the interacting $\pi$N pair. When the nonstatic $t$ matrix is averaged over the Fermi sea to obtain the optical potential, these frame transformation effects result in a substantial broadening of both pole and resonant contributions to the optical potential compared to the static optical potential.[9–12]

A self-consistent $\pi$-nuclear optical potential calculated with a nonstatic $t$ matrix is therefore expected to exhibit broadening due to the introduction of many-nucleon intermediate states and due to the transformation of the $t$ matrix from the $\pi$N center-of-mass frame to the nuclear rest frame. The first effect is dynamical in nature while the second is kinematical.

The object of this paper is to present an extension of the calculation presented in Ref. 1 by using a nonstatic $\pi$N $t$ matrix to calculate the self-consistent $\pi$N $t$ matrix in nuclear matter. This is motivated by the possibility that the kinematical broadening may tend to wash out the dynamical contribution. The present calculation shows that this is not the case. Indeed, all of the qualitative features of the static calculation are preserved in the nonstatic calculation.

In order to calculate a nonstatic self-consistent $t$ matrix, it is first necessary to obtain an expression for a free, nonstatic $\pi$N $t$ matrix expressed in the nuclear rest frame. Section II A outlines the derivation of a fully-off-shell, free $t$ matrix from field theoretical considerations.

The transformation properties of the $\pi$N $t$ matrix make it convenient to recast the self-consistent $t$-matrix equation in the form of two integral equations. These two equations, which express separately self-consistent modifications of the pole and cut contributions to the $t$ matrix, are presented in Sec. II B. The pole modifications are written in a form which emphasizes medium modifications to absorption vertices and nucleon propagation.

Section III A contains the details of a calculation of the nonstatic self-consistent $t$ matrix in nuclear matter along with the corresponding optical potential. The results of this calculation are presented in Sec. III B. Section IV presents a discussion of the calculations presented in this paper and states conclusions which may be drawn from this work.

## II. THEORY

### A. $\pi$N $t$ matrix

The fundamental building block of the organization of $\pi$-nucleus scattering as described in Ref. 1 is the free $\pi$N $t$ matrix. Since in this organization the $t$ matrix is used in constructing complex Goldstone diagrams which describe the scattering of the pion in the presence of nuclear excitations, a number of requirements must be imposed on the free $t$ matrix.

If the underlying theory describing the $\pi$N interaction is assumed to be a local relativistic field theory then the $\pi$N scattering amplitude is a Lorentz scalar function of six Lorentz scalar combinations of the three independent external momenta. These features of the amplitude are necessary to its use in the $\pi$-nucleus many-body problem for two reasons. The first is that since the $t$ matrix is to be used as an element in many-body diagrams, the squares of the pion and nucleon four-momenta will not, in general, be constrained by the usual mass shell condition, i.e., $k^2 \neq m_\pi^2$, $p^2 \neq m^2$, etc. The second reason is that in a Brueckner-Goldstone approach to the many-body problem the basis used to describe the nucleon states is an independent particle basis where the wave functions for these states are expressed in the nuclear rest frame. It is therefore convenient to express the $\pi$N $t$ matrix in this same frame. If the scattering amplitude is a Lorentz scalar function of Lorentz scalar combinations of the external four-momenta it is a trivial matter to express the $\pi$N $t$ matrix in any Lorentz frame.

The self-charge-conjugate nature of the pion implies that the $\pi$N $t$ matrix is symmetric under the crossing of the external pion lines which is equivalent to the interchange of variables $k \leftrightarrow -k'$ and $\alpha \leftrightarrow \beta$, where $k$ and $k'$ are the initial and final pion four-momenta and $\alpha$ and $\beta$ are the corresponding isospin indices. As a result of this symmetry the full $t$ matrix can be written as

$$T^0_{\pi N} = T^{0R}_{\pi N} + T^{0L}_{\pi N} ,$$

where the right-hand part $T^{0R}_{\pi N}$ and the left-hand part $T^{0L}_{\pi N}$ are related by the crossing of the external pion lines as illustrated in Fig. 1. Clearly the values of the right- and left-hand contributions as functions of the external variables will differ considerably.

Since it is not possible at this time to calculate the $\pi$N scattering amplitude from some basic theory such as quantum chromodynamics (QCD), it is necessary to use a

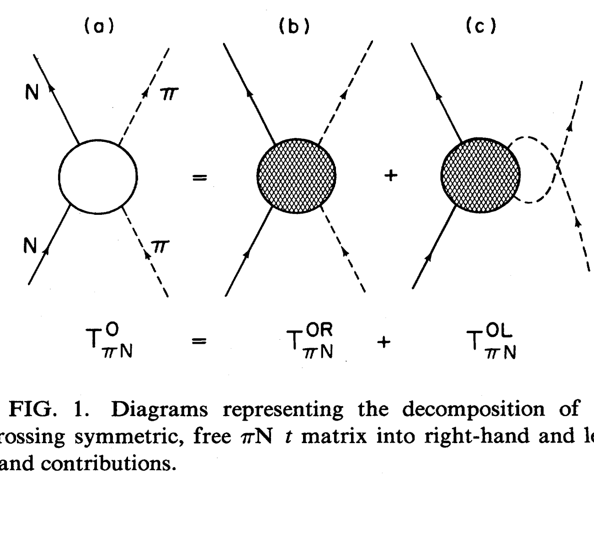


FIG. 1. Diagrams representing the decomposition of the crossing symmetric, free $\pi$N $t$ matrix into right-hand and left-hand contributions.

phenomenological representation of the offshell $\pi$N amplitude which respects the Lorentz transformation and crossing properties of the amplitude as far as possible. Such a phenomenological amplitude can be constructed by means of the Low expansion of the amplitude. As outlined below, half-off-mass-shell amplitudes parametrized in terms of experimentally determined forward scattering amplitudes and a form factor can be used to reduce the Low expanded amplitudes to a simple quadrature.[13]

For the energies considered in this paper the dominant contribution to the scattering amplitude is from the resonance in the $P33$ channel. Therefore, for the purpose of this paper, the discussion is specialized to the $P$-wave contributions to the amplitude although it may be generalized easily to include the $S$-wave contributions if a more accurate description of scattering near threshold is required. Since it involves little extra work, all $P$-wave cut contributions to the scattering amplitude (that is contributions associated with branch cuts in the amplitude) are retained in the calculations presented here. These contributions to the free $t$ matrix are represented by Fig. 2(c).

In order to obtain a reasonably complete physical description of $\pi$-nucleus scattering, the nucleon pole contribution to the $P11$ scattering must be included. This contribution in which a pion is absorbed and then remitted is represented by the diagram of Fig. 2(b). Inclusion of this contribution in the free $t$ matrix to be used in the many-nucleon problem will give rise to intermediate states where the pion is absorbed and one or more particle-hole pairs are excited.

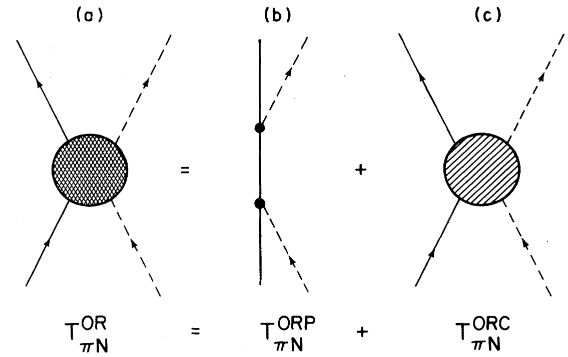


FIG. 2. Diagrams representing the decomposition of the right-hand cut contribution to the free $\pi$N $t$ matrix into pole and cut contributions.

From Eq. (39) of Ref. 13, the cut contribution to the $\pi$N scattering amplitude $F_{\beta\alpha}$ can be written as

$$F^{RC}_{\beta\alpha}=(2\pi)^3\sum_{\gamma}\sum_{s''}\int\frac{d^3k''}{(2\pi)^3 2\omega_{k''}}\int\frac{d^3p''}{(2\pi)^2}\frac{m}{E(p'')}\delta^{-3}(\vec{k}+\vec{p}-\vec{k}''-\vec{p}'')\times\frac{\langle p's'\,|\,j_\beta(0)\,|\,p''s'',k''\gamma\rangle\langle p''s'',k''\gamma\,|\,j_\alpha(0)\,|\,ps\rangle}{\omega_{k''}+E(p'')-k^0-p^0-i\eta}\,, \tag{1}$$

where $k$ and $p$ are the pion and nucleon four-momenta, $\alpha$ is the pion isospin index of the initial $\pi$N state, and $s$ is the spin of the nucleon. $k'$, $p'$, $\beta$, $s'$, and $k''$, $p''$, $\gamma$, $s''$ are the corresponding quantities for the final and intermediate states, respectively. It should be remembered that the intermediate states in the Low expansion are on-shell, asymptotic states with nucleon and pion energies $E(p'')=(\vec{p}\,''^2+m^2)^{1/2}$ and $\omega_{k''}=(\vec{k}\,''^2+m_\pi^2)^{1/2}$, where $m$ and $m_\pi$ are the nucleon and pion masses. If the initial and final state pions are allowed to be off mass shell, then the matrix elements of the pion source current operators $j_\alpha$ are half-off-shell matrix elements and the resultant amplitude $F^{RC}_{\beta\alpha}$ is fully off shell.

It should be noted that while the pions are off shell $(k^2\neq m^2,k'^2\neq m_\pi^2)$ in calculating these amplitudes the nucleons are not $(p^2=p'^2=m^2)$. It can be shown that using such amplitudes in the many-body problem is equivalent to neglecting components in the nuclear wave functions associated with nucleonic excitations having the same quantum numbers but larger mass than the nucleon such as the Roper resonance.[14]

Equation (1) is not covariant. This loss of covariance is the result of the truncation of the expansion in intermediate states to include only the $\pi$N intermediate state contribution to $F^{RC}_{\beta\alpha}$. The expansion can, of course, be carried out in any reference frame and one would expect that the physical importance of any particular intermediate state should not be dependent upon the choice of frame. For this reason, the noncovariance of Eq. (1) should not be a problem. Since the $\pi$N scattering amplitude will be used in conjunction with nuclear wave functions, it is most convenient to carry out the Low expansion in the nuclear rest frame. The various energies and momenta in (1) are therefore designated in the nuclear rest frame. The matrix elements of the pion source current are most conveniently expressed in the $\pi$N c.m. frame where a partial wave decomposition can be performed. The transformation between these two frames can be carried out by introducing the four-momentum

$$L=k+p=[(\vec{L}^2+W^2)^{1/2},\vec{L}]\,,$$

where $\vec{L}=\vec{k}+\vec{p}$ is the total three momentum of the $\pi$N pair and $W$ is the total c.m. energy or invariant mass of the intermediate state $\pi$N pair. For convenience, the total starting energy of the $\pi$N pair will be written as $\epsilon=k^0+p^0$. By a trivial use of the $\delta$ function, (1) can be rewritten as

$$F^{RC}_{\beta\alpha}=\frac{m}{2(2\pi)^3}\int\frac{d(W^2+\vec{L}^2)^{1/2}}{(W^2+\vec{L}^2)^{1/2}-\epsilon-i\eta}\times\left\{\sum_{\gamma}\sum_{s}\int\frac{d^3k''}{\omega_{k''}}\int\frac{d^3p''}{E(p'')}\delta^3(\vec{L}-\vec{k}''-\vec{p}'')\delta[(W^2+\vec{L}^2)^{1/2}-\omega_{k''}-E(\vec{p}'')]\right.$$
$$\left.\times\langle p's'|j_\beta(0)|p''s'',k''\gamma\rangle\langle p''s'',k''\gamma|j_\alpha(0)|ps\rangle\right\}. \quad (2)$$

The quantity enclosed in large curly brackets is an invariant and may therefore be calculated in any frame. The most convenient frame is obviously the $\pi$N c.m. frame where the pion source current matrix elements can be written in terms of the partial wave expansion

$$\langle -k''_{\text{c.m.}}s'',k''_{\text{c.m.}}\gamma|j_\alpha(0)|-k_{\text{c.m.}}s\rangle=4\pi\sum_{l,I,J}f^l_{2I,2J}(k''_{\text{c.m.}},k_{\text{c.m.}})\Pi^I(\gamma,\alpha)P^J_l(-\hat{k}''_{\text{c.m.}}s'',-\hat{k}_{\text{c.m.}}s)\ , \quad (3)$$

where $k_{\text{c.m.}}$ and $k''_{\text{c.m.}}$ are the pion initial and intermediate state four-momenta as measured in the center of mass of the intermediate state $\pi$N pair and $k_{\text{c.m.}}$ and $k''_{\text{c.m.}}$ are unit 3 vectors for this momenta. $l$, $I$, and $J$ are the orbital angular momentum, isospin, and total angular momentum labels of each partial wave. $f^l_{2I,2J}$ is the partial wave amplitude and $\Pi^I$ and $P^J_l$ are the isospin and angular momentum projection operators for each partial wave. Using expansion (3) along with the idempotency relations for the projectors

$$\sum_{s''}\int d\Omega_{k''_{\text{c.m.}}}[P^J_l(-\hat{k}''_{\text{c.m.}}s',-\hat{k}''_{\text{c.m.}}s'')P^{J'}_{l'}(-\hat{k}''_{\text{c.m.}}s'',-\hat{k}_{\text{c.m.}}s)]=\delta_{ll'}\delta_{JJ'}P^J_l(-\hat{k}'_{\text{c.m.}}s',-\hat{k}_{\text{c.m.}}s) \quad (4a)$$

and

$$\sum_{\gamma}\Pi^I(\beta,\gamma)\Pi^{I'}(\gamma,\alpha)=\delta_{I,I'}\Pi^I(\beta,\alpha)\ , \quad (4b)$$

Eq. (2) becomes

$$F_{\beta\alpha}=\frac{m}{\pi}\int\frac{d(W^2+\vec{L}^2)^{1/2}}{(W^2+\vec{L}^2)^{1/2}-\epsilon-i\eta}\times\left\{\sum_{l,I,J}\int_0^\infty\frac{dk''_{\text{c.m.}}k''^2_{\text{c.m.}}}{\omega_{k''_{\text{c.m.}}}E(\vec{k}''_{\text{c.m.}})}\delta[W-\omega_{k''_{\text{c.m.}}}-E(k''_{\text{c.m.}})]\right.$$
$$\left.\times f^{l*}_{2I,2J}(k''_{\text{c.m.}},k'_{\text{c.m.}})f^l_{2I,2J}(k''_{\text{c.m.}},k_{\text{c.m.}})\Pi^I(\beta,\alpha)P^J_l(-\hat{k}'_{\text{c.m.}}s',-\hat{k}_{\text{c.m.}}s)\right\}. \quad (5)$$

The half-off-mass shell amplitudes can be parametrized by a factorable form,

$$f^l_{2I,2J}(q,p)=\frac{|\vec{p}|}{|\vec{q}|}\frac{\phi(p)}{\phi(q)}f^l_{2I,2J}(q,q)\ , \quad (6)$$

where $\phi$ is a form factor and the forward on-shell elastic scattering amplitude $f^l_{2I,2J}(q,q)$ can be written in terms of measured phase shifts as

$$f^l_{2I,2J}(q,q)=-\frac{4\pi W}{m}\frac{1-\eta^l_{2I,2J}e^{2i\delta^l_{2I,2J}}}{2iq}\ . \quad (7)$$

This along with the condition for elastic unitarity,

$$\text{Im}f^l_{2I,2J}(k''_{\text{c.m.}},k'_{\text{c.m.}})=\frac{mk''_{\text{c.m.}}}{4\pi W}|f^l_{2I,2J}(k''_{\text{c.m.}},k''_{\text{c.m.}})|^2\ , \quad (8)$$

can be used to write the fully off-shell amplitude as

$$F^{RC}_{\beta\alpha}=4\int\frac{d(W^2+\vec{L}^2)^{1/2}}{(W^2+\vec{L}^2)^{1/2}-\epsilon-i\eta}\frac{|\vec{k}'_{\text{c.m.}}||\vec{k}_{\text{c.m.}}|}{|\vec{k}''_{\text{c.m.}}|^2}\frac{\phi(k'_{\text{c.m.}})\phi(k_{\text{c.m.}})}{\phi^2(k''_{\text{c.m.}})}$$
$$\times\sum_{l,I,J}\Pi^I(\beta,\alpha)P^J_l(-k'_{\text{c.m.}}s',-k_{\text{c.m.}}s)\text{Im}f^l_{2I,2J}(k''_{\text{c.m.}},k''_{\text{c.m.}})\ . \quad (9)$$

The external momenta $k$ and $k'$ are expressed here in the $\pi$N c.m. frame rather than the nuclear rest frame as desired. By again using the four-momentum $L$, the $p$-wave projection operators can be written in an arbitrary frame as

$$P_1^{1/2}(\hat{p}'s,\hat{p}s)=\frac{m}{4\pi}\frac{\bar{u}(p's')\left[\dfrac{\gamma\cdot L}{m}-1\right]u(ps)}{\{[E(p)-m][E(p')-m]\}}\,, \tag{10a}$$

$$P_1^{3/2}(\hat{p}s',\hat{p}s)=-\frac{m}{4\pi}\frac{\bar{u}(p's')3\left[1+\dfrac{\gamma\cdot L}{W}\right]u(ps)}{\{[E(p)-m][E(p')-m]\}^{1/2}}\frac{\left[p'\cdot p+\dfrac{p'\cdot Lp\cdot L}{W^2}\right]}{[E(p)+m][E(p')+m]}-P_1^{1/2}(p's,ps)\,, \tag{10b}$$

and

$$\vec{k}^{\,2}_{\text{c.m.}}=-\left[p^2+\frac{(p\cdot L)^2}{W^2}\right],\qquad \vec{k}'^{\,2}_{\text{c.m.}}=-\left[p'^2+\frac{(p'\cdot L)^2}{W^2}\right]. \tag{11}$$

If it is assumed that the momenta $p$, $p'$, and $\vec{L}$ are much smaller than the masses $m$ and $W$, Eq. (9) along with Eqs. (10) and (11) can be expanded in powers of momentum over mass. Keeping only terms up to first order in the expansion, the scattering amplitude may be written as

$$F^{RC}_{\beta\alpha}\cong 4\int_{m+\mu}^{\infty}\frac{dW}{W+\dfrac{L^2}{2W}-\epsilon-i\eta}\frac{\phi(k'_{\text{c.m.}})\phi(k_{\text{c.m.}})}{\phi^2(k''_{\text{c.m.}})}\times\sum_{l,I,J}\text{Im}h^l_{2I,2J}(W)\xi^\dagger_{t'}\Lambda_{2I}(\beta,\alpha)\times\xi_t\chi^\dagger_{s'}\Omega^l_{2J}(\vec{k}'_{\text{c.m.}},\vec{k}_{\text{c.m.}})\chi_s\,, \tag{12}$$

where the definitions

$$f^l_{2I,2J}(k''_{\text{c.m.}},k''_{\text{c.m.}})=4\pi k''^2_{\text{c.m.}}(W)h^l_{2I,2J}(W)\,, \tag{13a}$$

$$\Pi^I(\beta,\alpha)=\xi^\dagger_{t'}\Lambda_{2I}(\beta,\alpha)\xi_t\,, \tag{13b}$$

and

$$4\pi k'_{\text{c.m.}}k_{\text{c.m.}}P^l_{2J}(-k'_{\text{c.m.}}s',-k_{\text{c.m.}}s)=\chi^\dagger_{s'}\Omega^l_{2J}(\vec{k}''_{\text{c.m.}},\vec{k}_{\text{c.m.}})\chi_s \tag{13c}$$

have been used. The $\pi$N c.m. momenta are related to the nuclear rest frame momenta by

$$\vec{k}'_{\text{c.m.}}=-\left[\vec{p}\,'-\frac{m}{W}\vec{L}\right]=\vec{k}\,'-\frac{W-m}{W}\vec{L} \tag{14a}$$

and

$$\vec{k}_{\text{c.m.}}=-\left[\vec{p}-\frac{m}{W}\vec{L}\right]=\vec{k}-\frac{W-m}{W}\vec{L}\,. \tag{14b}$$

The $P$-wave angular momentum projection operators and isospin $\frac{1}{2}$ and $\frac{3}{2}$ projection operators are

$$\Omega'_1(\vec{k}'_{\text{c.m.}},\vec{k}_{\text{c.m.}})=\vec{\sigma}\cdot\vec{k}'_{\text{c.m.}}\vec{\sigma}\cdot\vec{k}_{\text{c.m.}}\,,\qquad \Omega'_3(\vec{k}'_{\text{c.m.}},\vec{k}_{\text{c.m.}})=3\vec{k}'_{\text{c.m.}}\cdot\vec{k}_{\text{c.m.}}-\Omega'_1(\vec{k}'_{\text{c.m.}},\vec{k}_{\text{c.m.}})\,, \tag{15a}$$

$$\Lambda_1(\beta,\alpha)=\tfrac{1}{3}\tau_\beta\tau_\alpha\,,\qquad \Lambda_2(\beta,\alpha)=\delta_{\beta\alpha}-\Lambda_1(\beta,\alpha)\,. \tag{15b}$$

The $\tau_\alpha$'s are the usual Pauli matrices and $\xi_t$ and $\chi_s$ are the isospin and spin Pauli spinors.

The amplitude described by (12) can be further simplified by replacing the invariant mass $W$ in the recoil energy contribution to the denominator $L^2/2W$ and in (14) by the resonant mass $m_\Delta$. In principle, this should be the mass of the lowest resonance in each channel but since the amplitude is dominated by the $P33$ amplitude in the region of interest, the mass of the $\Delta$ is used here to describe the recoil mass in all channels. Equation (14) now becomes

$$\vec{k}'_{\text{c.m.}}=\vec{k}\,'-\delta\vec{L}\,,\qquad \vec{k}_{\text{c.m.}}=\vec{k}-\delta\vec{L}\,, \tag{16}$$

where $\delta=(m_\Delta-m)/m_\Delta$. An off-shell partial wave amplitude can now be identified as

$$h^{0IRC}_{2I,2J}\left[\epsilon-\frac{L^2}{2m_\Delta}\right]=-\frac{1}{\pi}\int_{m+\mu}^{\infty}\frac{dW\,\phi^{-2}(k''_{\text{c.m.}})\text{Im}h^l_{2I,2J}(W)}{\epsilon-\dfrac{L^2}{2m_\Delta}-W+i\eta}\,. \tag{17}$$

The right-hand cut contribution to the free $t$ matrix can be written as

$$\hat{T}^{0RC}_{\pi\text{N}}(k'\beta,k\alpha;p',p)=-4\pi\sum_{l,I,J}h^{0IRC}_{2I,2J}\left[\epsilon-\frac{L^2}{2m_\Delta}\right]\Lambda_{2I}(\beta,\alpha)\Omega^l_{2J}(\vec{k}'_{\text{c.m.}},\vec{k}_{\text{c.m.}})\frac{\phi(k'_{\text{c.m.}})\phi(k_{\text{c.m.}})}{\sqrt{2\omega_{k'}}\sqrt{2\omega_k}}\,. \tag{18}$$

This $t$ matrix is an operator in the spin-isospin space of the nucleons.

From Ref. 14, Eqs. (19) and (20), the right-hand nucleon pole contribution to the amplitude can be written as

$$F^{RP}_{\beta\alpha} = +\frac{1}{2m} g_\pi[(p'-L)^2] g_\pi[(p-L)^2] \xi^\dagger_{t'} \times \frac{\bar{u}(p's')\gamma_5\tau_\beta(\gamma\cdot L+m)\gamma_5\tau_\alpha u(ps)}{\epsilon-(\vec{L}^2+m^2)^{1/2}+i\eta}\xi_t \ ,$$

where $L=[(\vec{L}^2+m^2)^{1/2},\vec{L}]$ is the four-momentum of the on-shell intermediate state nucleon. This may be simplified to yield

$$F^{RP}_{\beta\alpha} = \frac{g_\pi[(p'-L)^2] g_\pi[(p-L)^2]}{2m} \times \frac{\bar{u}(p's')(-\gamma\cdot L+m)u(ps)}{\epsilon-E(\vec{L})+i\eta}\xi^\dagger_{t'}\tau_\beta\tau_\alpha\xi_t \ . \tag{19}$$

If the momenta are assumed to be small compared to the nucleon mass, (19) reduces to

$$F^{RP}_{\beta\alpha} \cong -\frac{3g_\pi^2(0)}{4m^2}\phi(k')\phi(k)\frac{\Omega_1'(\vec{k}',\vec{k})\Lambda_1(\beta,\alpha)}{\epsilon-\frac{L^2}{2m}-m+i\eta} \ , \tag{20}$$

where the form factor has been written as

$$g_\pi[(p-L)^2] = g_\pi(0)\phi[(p-L)^2] \ ,$$
$$g_\pi(0) = \sqrt{2}\frac{m m_\pi^2 g_A(0)}{f_\pi} \ . \tag{21}$$

The pole contribution to the free $t$ matrix can be written as

$$\hat{T}^{0RP}_{\pi N}(k'\beta,k\alpha;p',p) = -4\pi h^{0RP}\left[\epsilon-\frac{L^2}{2m}\right]\Lambda_1(\beta,\alpha)\Omega_1'(\vec{k}',\vec{k}) \times \frac{\phi(k')\phi(k)}{\sqrt{2\omega_{k'}}\sqrt{2\omega_k}} \ , \tag{22}$$

where

$$h^{0RP}\left[\epsilon-\frac{L^2}{2m}\right] = -\frac{3g_\pi^2(0)}{16\pi m^2}\frac{1}{\epsilon-\frac{L^2}{2m}-m+i\eta} \ . \tag{23}$$

Note that the pion momenta appearing in the angular momentum projection operators are those measured in the nuclear rest frame. This is consistent with the recoil mass of the intermediate state of the pole term being the nucleon mass $m$. This can be seen by making the substitution $m_\Delta \to m$ in Eq. (16). The crossed amplitudes can be obtained by simply applying the crossing relations to (18) and (22).

### B. The self-consistent $t$ matrix

In the previous subsection, expressions were derived for the pole and cut contributions to the free $t$ matrix in the nuclear rest frame. Because of the difference in mass of the intermediate states of these two contributions, the effects of the transformation from $\pi$N c.m. frame to nuclear rest frame result in different recoil energies and angle transformations in the angular momentum projection operators for the pole and cut contributions. For this reason, it is convenient also to separate the self-consistent $\pi$N $t$ matrix into a pole and a cut contribution. Once this separation is made it is instructive to rearrange the pole contribution to the self-consistent $t$ matrix in a manner which emphasizes the physical meaning of the modifications to the nucleon pole term in the nuclear medium. The self-consistent $t$ matrix satisfies the equation

$$T_{\pi N} = T^0_{\pi N} + T^0_{\pi N}\left[\frac{Q}{E-K_\pi-K_N-\Sigma(\omega-K_N)+i\eta} - \frac{1}{E-K_\pi-K_N+i\eta}\right]T_{\pi N} \ , \tag{24}$$

where $T^0_{\pi N}$ is the free $\pi$N $t$ matrix, $T_{\pi N}$ is the self-consistent $\pi$N $t$ matrix, $Q$ is the Pauli operator which projects onto unoccupied nucleon states, $E$ is the starting energy of the $\pi$N pair, $K_\pi=(m_\pi^2-\nabla_\pi^2)^{1/2}$, and $K_N=-\nabla_N^2/2m$. The first term inside of the large brackets is the $\pi$N propagator where the nucleon is restricted to unoccupied states and the $\pi$ propagates in the presence of an optical potential given by the $\pi$ self-energy $\Sigma$. For the present, the optical potential for the nucleon is ignored. The second term in large brackets is the free $\pi$N propagator. The effective $t$ matrix given by the self-consistent equation can therefore be viewed as the free $t$ matrix plus terms which correct for Pauli blocking and pion distortion in intermediate states of the $t$ matrix in the presence of the nuclear medium. The self-consistency arises because the $\pi$ self-energy $\Sigma$ is calculated by taking the nuclear ground state matrix element of the self-consistent $t$ matrix

$$\Sigma = \langle\psi_0|T_{\pi N}|\psi_0\rangle \ . \tag{25}$$

This is represented by the diagrams in Fig. 3 where the cross-hatched circle represents the free $\pi$N $t$ matrix, the cross-hatched box represents the self-consistent $t$ matrix, upward going solid lines represent particles, downward-going solid lines represent holes, dashed lines represent free pion propagation, and double dashed lines represent pion propagation in the presence of an optical potential. In general, the free and self-consistent $t$ matrices in (24) and (25) contain both left- and right-hand contributions. For the purpose of the following discussion only the right-hand pole and cut contributions are included. Inclusion of the crossed amplitudes will be discussed in a subsequent paper.

The right-hand contribution to the free $t$ matrix can be written as the sum of a pole and a cut contribution

$$T^{0R}_{\pi N} = T^{0RP}_{\pi N} + T^{0RC}_{\pi N} \tag{26}$$

as illustrated in Fig. 2. In a similar fashion the self-consistent $x$ matrix can be separated into pole and cut contributions

$$T^R_{\pi N} = T^{RP}_{\pi N} + T^{RC}_{\pi N} \tag{27}$$

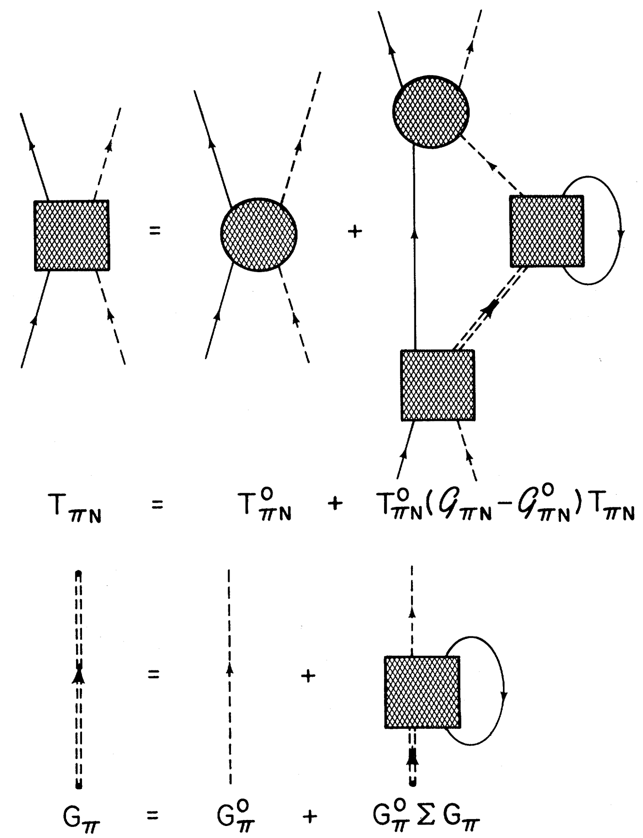


FIG. 3. Diagrammatic representation of the self-consistent $t$-matrix equations.

as illustrated in Fig. 4 where the hatched line represents the self-consistent nucleon pole and the hatched box represents the self-consistent right-hand cut.

The self-consistent equation (24) can now be divided into two integral equations:

$$T^{RC}_{\pi N}=T^{0RC}_{\pi N}+T^{0RC}_{\pi N}(\mathcal{G}_{\pi N}-\mathcal{G}^{0}_{\pi N})T^{RC} \tag{28a}$$

and

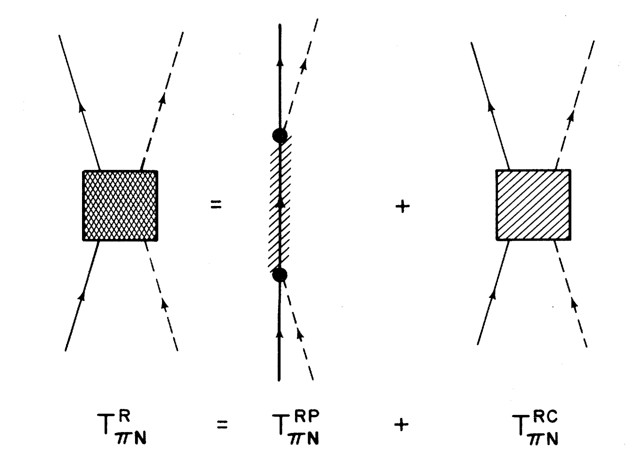


FIG. 4. Diagrams representing the decomposition of the right-hand cut contribution to the self-consistent $t$ matrix into pole and cut contributions.

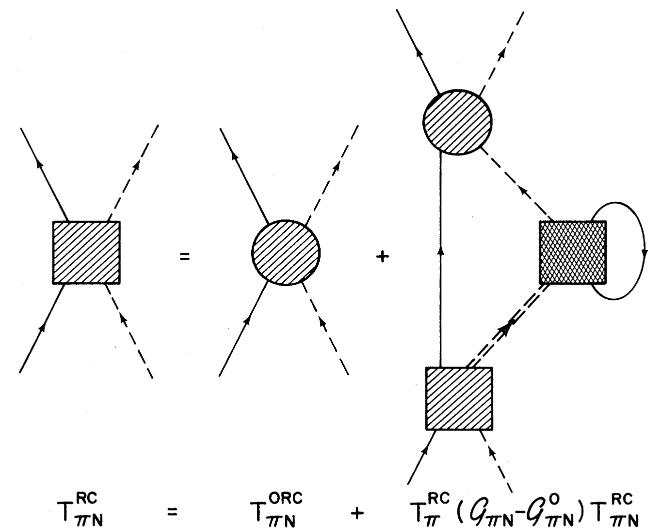


FIG. 5. Diagrammatic representation of the equation for the right-hand cut contribution to the self-consistent $t$ matrix.

$$T^{RP}_{\pi N}=T^{0RP}_{\pi N}+T^{0RP}_{\pi N}(\mathcal{G}_{\pi N}-\mathcal{G}^{0}_{\pi N})T^{RC}_{\pi N}+T^{0RC}_{\pi N}(G-G_0)T^{RP}+T^{0RP}_{\pi N}(\mathcal{G}_{\pi N}-\mathcal{G}^{0}_{\pi N})T^{RP}_{\pi N}\ , \tag{28b}$$

which are represented by the diagrams of Figs. 5 and 6. This separation is made so that (28a) contains no pieces which contain a single nucleon pole. Note that (28a) has the same form as the full self-consistent equation (24). The full self-consistent $t$-matrix equation (24) is recovered by simply adding (28a) and (28b).

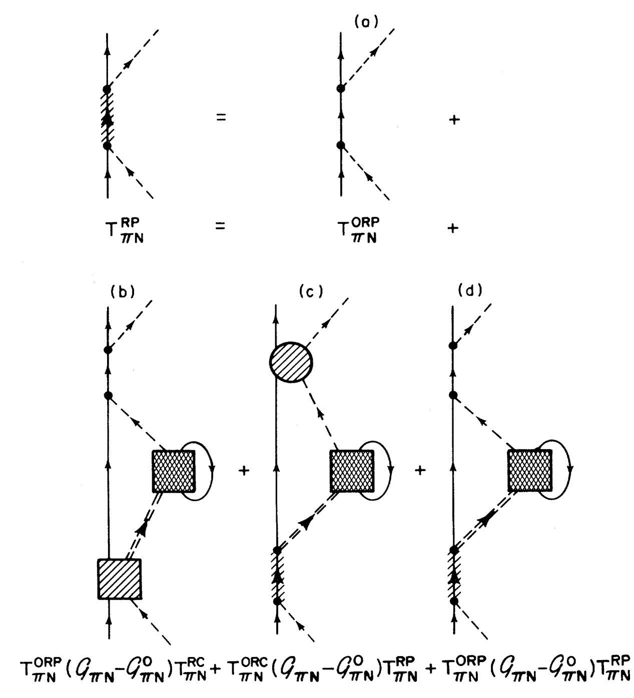


FIG. 6. Diagrammatic representation of the equation for the right-hand cut contribution to the self-consistent $t$ matrix.

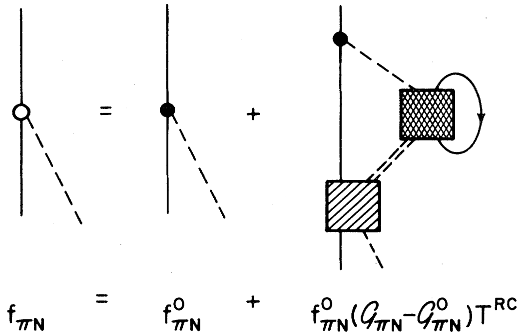


FIG. 7. Diagrammatic representation for the effective $\pi$NN vertex in the nuclear medium.

It is useful to rewrite (28b) in a form which better illustrates the meaning of the self-consistent modifications to the nucleon pole contribution. This reorganization is suggested by considering the diagrams of Fig. 6. Figures 6(b) and 6(c) suggest a medium modification to the pion absorption vertex while Fig. 6(d) suggests a nucleon self-energy insertion. The self-consistent pion absorption vertex can be written as

$$f_{\pi N}=f^{0}_{\pi N}+f^{0}_{\pi N}(\mathcal{G}_{\pi N}-\mathcal{G}^{0}_{\pi N})T^{RC}_{\pi N}\ , \tag{29}$$

where $f^{0}_{\pi N}$ is the free pion-nucleon absorption vertex and $f_{\pi N}$ is the corresponding self-consistent vertex. The equation is represented by the diagrams of Fig. 7 where the solid dot represents the free vertex and the empty dot, the self-consistent vertex. A similar equation can be written for the pion emission vertex,

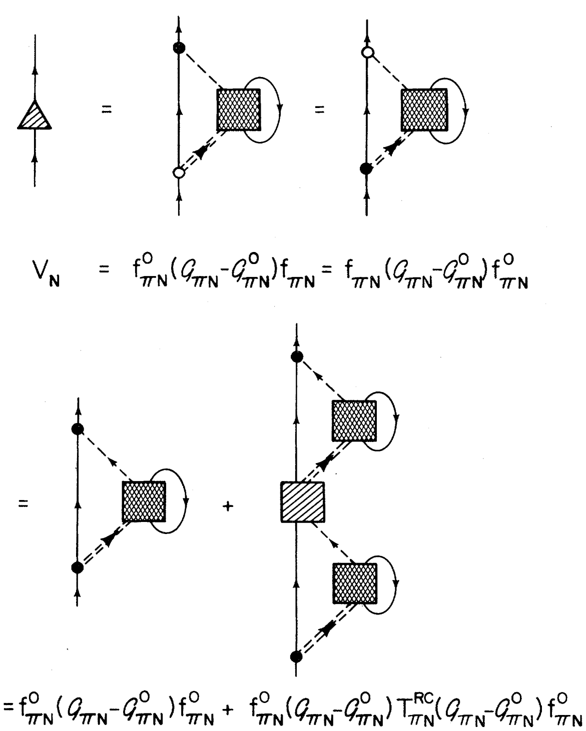


FIG. 8. Diagrammatic representation of the contributions to the nucleon optical potential generated by the self-consistent $t$-matrix equation.

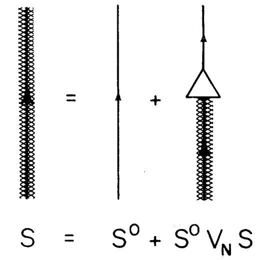


FIG. 9. Diagrammatic representation of the dressed nucleon propagator.

$$f_{\pi N}=f^{0}_{\pi N}+T^{RC}_{\pi N}(\mathcal{G}_{\pi N}-\mathcal{G}^{0}_{\pi N})f^{0}_{\pi N}\ , \tag{30}$$

which is represented by the time-reversed diagrams corresponding to those of Fig. 7. A nucleon self-energy can be defined as

$$\begin{aligned}V_{N}&=f^{0}_{\pi N}(\mathcal{G}_{\pi N}-\mathcal{G}^{0}_{\pi N})f_{\pi N}=f_{\pi N}(\mathcal{G}_{\pi N}-\mathcal{G}^{0}_{\pi N})\\&=f^{0}_{\pi N}(\mathcal{G}_{\pi N}-\mathcal{G}^{0}_{\pi N})f^{0}_{\pi N}\\&\quad+f^{0}_{\pi N}(\mathcal{G}_{\pi N}-\mathcal{G}^{0}_{\pi N})T^{RC}_{\pi N}(\mathcal{G}_{\pi N}-\mathcal{G}^{0}_{\pi N})f^{0}_{\pi N}\ ,\end{aligned} \tag{31}$$

which is represented by the diagrams of Fig. 8, where the hatched triangle represents the nucleon self-energy. Using this nucleon self-energy, a dressed nucleon propagator can be defined as

$$S=S^{0}+S^{0}V_{N}S\ , \tag{32}$$

where $S^0$ is the free nucleon propagator and $S$ is the dressed nucleon propagator. This equation is represented by Fig. 9 where the cross-hatched line represents the dressed nucleon propagator and the solid line, the free nucleon propagator.

In the notation used above, the pole contribution to the free $t$ matrix can be written as

$$T^{0RP}=f^{0}_{\pi N}S^{0}f^{0}_{\pi N}\ , \tag{33}$$

while the pole contribution to the self-consistent $t$ matrix can now be written as

$$T^{RP}=f_{\pi N}Sf_{\pi N}\ , \tag{34}$$

which is represented by Fig. 10. This can be verified by

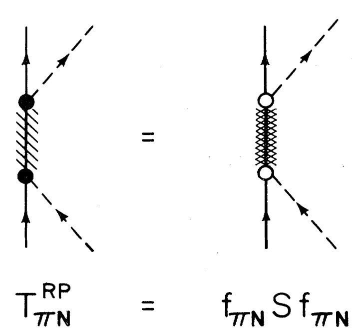


FIG. 10. Diagrammatic representation of the right-hand pole contribution to the self-consistent $t$ matrix expressed in terms of medium modified pion absorption and emission vertices and the dressed nucleon propagator.

simply substituting (29), (30), (31), and (32) into (34) to reproduce (28b).

It is necessary to make some comment about the nucleon self-energy defined by (31). It should be remembered that the diagrams used to define the quantity above are time-ordered Goldstone diagrams where upward-going nucleon lines represent particles above the Fermi sea while downward-going nucleon lines represent holes in the Fermi sea. The nucleon self-energy defined by (31) acts only on particles above the Fermi sea and therefore corresponds to an optical potential for nucleons in excited states. This is a rather unusual collection of contributions to the nucleon optical potential and will have little resemblence to phenomenological optical potentials. In addition, if a realistic optical potential is used to provide wave functions for particle states in the Goldstone treatment of the nuclear many-body problem, the nucleon self-energy generated as part of the self-consistent $\pi$N $t$ matrix will double count certain contributions to the realistic optical potential. If the dressing of particle lines is important to the calculation, the optical potential used for this purpose should be used to generate $S$ in (34) rather than the self-energy given by (31).

## III. CALCULATIONS

### A. The self-consistent $t$ matrix in nuclear matter

Now that a model for the fully-off-shell free $\pi$N $t$ matrix has been presented along with a statement of the self-consistent equations, the self-consistent $t$ matrix can be calculated once a model for the nuclear wave function is provided. The difficulty in solving these equations for finite nuclei can be appreciated by noticing that the self-consistent $t$ matrix equations are basically three body in nature since they involve the interaction of a pion, a valence nucleon, and the residual nuclear core. Given the large number of partial waves required to describe the scattering of the pion from the nuclear core, it is not clear whether such a calculation is presently possible.

The qualitative features of the self-consistent $t$ matrix can be studied, however, by calculating it in nuclear matter where the nuclear wave functions are plane waves and the pion is elastically scattered only in the forward direction. This was the approach of the "simple solvable model" calculation of Ref. 1. The simplicity of this calculation was obtained at the expense of using a static model for the free $\pi$N $t$ matrix which corresponds to setting $\vec{L}=0$ in (16), (18), and (22). By doing this, the Fermi motion and angle transformation effects due to the frame transformation are suppressed. This results in a pion self-energy which fails to contain the nonlocalities associated with intermediate state propagation. Another serious defect arises from the fact that the nucleon pole contribution to the $t$ matrix is represented by a simple pole as a function of the pion energy, which translates to a similar simple pole in the self-energy.

In nuclear matter, the equation for the right-hand cut contribution to the self-consistent $t$ matrix (28a) can be written as

$$\hat{T}^{RC}_{\pi\mathrm{N}}(k'\beta,k\alpha;p',p)=\hat{T}^{0RC}_{\pi\mathrm{N}}(k'\beta,k\alpha;p',p)+\frac{1}{(2\pi)^3}\sum_{\gamma}\int d^3q\,\hat{T}^{0RC}_{\pi\mathrm{N}}(k'\beta,q\gamma,p',L-q)$$
$$+\left\{\frac{\theta(|\vec{L}-\vec{q}|-k_F)}{\epsilon-E(\vec{L}-\vec{q})-\omega_q-\Sigma[\vec{q},\epsilon-E(L-q)]+i\eta}-\frac{1}{\epsilon-E(\vec{L}-\vec{q})-\omega_q+i\eta}\right\}\hat{T}^{RC}_{\pi\mathrm{N}}(q\gamma,k\alpha;p',p)\;, \tag{35}$$

where $\hat{T}^{0RC}_{\pi\mathrm{N}}$ is given by (18), $E(p)\cong m+p^2/2m$, and

$$\epsilon=\omega-B+E(p)$$

is the starting energy of the $\pi$N pair, $B$ represents an average nuclear binding energy in nuclear matter, and $k_F$ is the Fermi momentum and $E(P)=p^2/2m$. As an ansatz, the self-consistent right-hand-cut $t$ matrix is assumed to have the form

$$\hat{T}^{RC}_{\pi\mathrm{N}}=-4\pi\sum_{I,J}h^{RC}_{2I,2J}\left[\epsilon-\frac{L^2}{2m_\Delta},L\right]\Lambda_{2I}(\beta,\alpha)\Omega_{2J}(\vec{k}'_{\mathrm{c.m.}},\vec{k}_{\mathrm{c.m.}})\frac{\phi(\vec{k}'_{\mathrm{c.m.}})}{\sqrt{2\omega_{k'}}}\frac{\phi(\vec{k}_{\mathrm{c.m.}})}{\sqrt{2\omega_k}}\;, \tag{36}$$

which is of the same form as (18) with the modification that the amplitude $h^{RC}_{2I,2J}$ may now have some extra dependence on the total pair momentum $L$.

For the purpose of simplifying the calculation, two approximations are introduced. The first is that the spin flip contributions to the angular momentum projection operators are neglected, that is

$$\Omega_{2J}(\vec{k}'_{\mathrm{c.m.}},\vec{k}_{\mathrm{c.m.}})\cong(J+1/2)\vec{k}'_{\mathrm{c.m.}}\cdot\vec{k}_{\mathrm{c.m.}}\;. \tag{37}$$

By dropping such terms, the complexity of the coupling between various spin-isospin channels is greatly reduced. This should not seriously change the qualitative results of the calculation. The second modification is to replace the center-of-mass momentum in the off-shell form factors by the pion momentum in the nuclear rest frame,

$$\phi(k_{\mathrm{c.m.}})\cong\phi(k)\ .$$

Since the primary effect of the form factor in this calculation is to act as a cutoff in the internal loop momentum integrals, this should have no qualitative effect on the results of the calculation.

For this calculation, the form factors are chosen to be of a Gaussian form,

$$\phi(k)=e^{-\vec{k}^2/\mu^2}\ , \tag{38}$$

where $\mu$ is the form factor mass.

With these approximations and using the idempotency relation for the isospin operators (4a), the self-consistent equation (35) can be separated into expressions for each isospin channel and becomes

$$\vec{k}'_{\mathrm{c.m.}}\cdot\vec{k}_{\mathrm{c.m.}}H_{2I}^{RC}\left[\epsilon-\frac{L^2}{2m_\Delta},L\right]=\vec{k}'_{\mathrm{c.m.}}\cdot\vec{k}_{\mathrm{c.m.}}H_{2I}^{0RC}\left[\epsilon-\frac{L^2}{2m_\Delta}\right]-H_{2I}^{0RC}\left[\epsilon-\frac{L^2}{2m_\Delta}\right]f(\epsilon,\vec{k}'_{\mathrm{c.m.}},\vec{k}_{\mathrm{c.m.}},\vec{L})H_{2I}^{RC}\left[\epsilon-\frac{L^2}{2m_\Delta},L\right]\ , \tag{39}$$

where

$$H_{2I}^{0RC}=4\pi\sum_J(J+1/2)h_{2I,2J}^{0RC}\ ,$$

$$H_{2I}^{RC}=4\pi\sum_J(J+1/2)h_{2I,2J}^{RC}\ ,$$

and

$$f(\epsilon,\vec{k}'_{\mathrm{c.m.}},\vec{k}_{\mathrm{c.m.}},\vec{L})=\frac{1}{2(2\pi)^3}\int\frac{d^3q}{\omega_q}\phi^2(q)\vec{k}'_{\mathrm{c.m.}}\cdot\vec{q}_{\mathrm{c.m.}}\vec{q}_{\mathrm{c.m.}}\cdot\vec{k}_{\mathrm{c.m.}}$$
$$\times\left\{\frac{\theta(|\vec{L}-\vec{q}\,|-k_F)}{\epsilon-E(\vec{L}-\vec{q})-\omega_q-\Sigma[\vec{q},\epsilon-E(L-q)]+i\eta}-\frac{1}{\epsilon-E(\vec{L}-\vec{q})-\omega_q+i\eta}\right\}\ . \tag{40}$$

The function $f$, in general, contains contributions to many partial waves. Here, we are only interested in the $P$-wave contribution. Therefore, only the part of $f$ proportional to $\vec{k}'_{\mathrm{c.m.}}\cdot\vec{k}_{\mathrm{c.m.}}$ and independent of the direction of $\vec{L}$ is retained. It is then possible to rewrite (39) as

$$H_{2I}^{RC}\left[\epsilon-\frac{L^2}{2m_\Delta},L\right]=H_{2I}^{0RC}\left[\epsilon-\frac{L^2}{2m_\Delta}\right]-H_{2I}^{0RC}\left[\epsilon-\frac{L^2}{2m_\Delta}\right]F(\epsilon,L)H_{2I}^{RC}\left[\epsilon-\frac{L^2}{2m_\Delta},L\right]\ , \tag{41}$$

where

$$F(\epsilon,L)=\frac{m}{16\pi^2L}\int_0^\infty\frac{dq\,q}{\omega_q}\phi^2(q)\int_{-\infty}^{\infty}d\mathscr{E}\left\{\frac{\theta(\epsilon-\mathscr{E}-\epsilon_F)}{\mathscr{E}-\omega_q-\Sigma(q,\mathscr{E})+i\eta}-\frac{1}{\mathscr{E}-\omega_q+i\eta}\right\}(1-u_0^2)\theta(1+u_0)\theta(1-u_0)\ , \tag{42}$$

where

$$u_0=\frac{mW}{qL}\ ,$$

and

$$W=\mathscr{E}-\epsilon+E(L)+E(q)-m\ .$$

The self-consistent $H$ amplitude is now found by a simple algebraic solution of (41) as

$$H_{2I}^{RC}\left[\epsilon-\frac{L^2}{2m_\Delta},L\right]=\frac{1}{H_{2I}^{0RC^{-1}}\left[\epsilon-\dfrac{L^2}{2m_\Delta}\right]+F(\epsilon,L)}\ . \tag{43}$$

A similar procedure can be used to solve (28b) for the self-consistent pole contribution. This gives

$$H_1^{RP}\left[\epsilon-\frac{L^2}{2m},L\right]=\frac{4\pi h^{0RP}(\epsilon-L^2/2m)}{1+\left[H_1^{0RC}\left[\epsilon-\dfrac{L^2}{2m_\Delta}\right]+4\pi h^{0RP}\left[\epsilon-\dfrac{L^2}{2m}\right]F(\epsilon,L)\right]}\left[1-F(\epsilon,L)H_1^{RC}\left[\epsilon-\frac{L^2}{2m_\Delta},L\right]\right]\ , \tag{44}$$

where $F$ is again defined by (42). Using (43) this can be rewritten in a form which is more suggestive of the alternate form of the pole contribution to the self-consistent $t$ matrix (34),

$$H_1^{RP}\left[\epsilon-\frac{L^2}{2m},L\right]=\frac{1}{1+\left[H_1^{0RC}\left[\epsilon-\frac{L^2}{2m_\Delta}\right]F(\epsilon,L)\right]}\,\frac{4\pi h^{0RP}\left[\epsilon-\frac{L^2}{2m}\right]}{1+4\pi h^{0RP}\left[\epsilon-\frac{L^2}{2m}\right]\left[\frac{F(\epsilon,L)}{1+H_1^{0RC}\left[\epsilon-\frac{L^2}{2m_\Delta}\right]F(\epsilon,L)}\right]}$$

$$\times\frac{1}{1+H_1^{0RC}\left[\epsilon-\frac{L^2}{2m_\Delta}\right]F(\epsilon,L)}\,. \tag{45}$$

Therefore, both pole and cut contributions to the self-consistent $t$ matrix can be found easily once the function $F(\epsilon,L)$ defined by (42) is known. To calculate $F$, it is necessary to have an expression for the self-energy $\Sigma$, which in principle should be calculated from the self-consistent $t$ matrix, which we are trying to find. A practical approach to this self-consistency problem is to iterate in approximations to $\Sigma$. This is done by first calculating $\Sigma^0$ which is calculated from the free $t$ matrix. This can then be used in (42), (43), and (44) to provide an estimate of the self-consistent $t$ matrix which can be used to provide a new estimate of $\Sigma$. This procedure is continued until there is little variation in successive estimates of $T_{\pi N}$. The static $t$-matrix calculation of Ref. 1 showed this to be a very rapidly convergent procedure. Indeed, it was found that a good estimate of the converged result was obtained by the initial calculation using $\Sigma=\Sigma^0$. For this reason, this approximation with some modification is used in the results presented below. Self-consistency can, of course, be obtained by iteration, but this should provide no qualitative changes in the result.

Before simply using $\Sigma^0$ in the calculation of $F$, some thought needs to be given to the effect of Pauli blocking on the self-energy. The effect of Pauli blocking on the resonant contribution to $\Sigma$ is to shift the energy and narrow the resonance by excluding a portion of the phase space available to intermediate state nucleons. These effects are in the opposite direction to those which form the introduction of the many-nucleon degrees of freedom which provide a downward shift and a broadening of the resonance. Therefore, the cut contribution to the self-energy calculated from the free $t$ matrix is actually a better approximation to the self-consistent self-energy than is the Pauli corrected self-energy. The Pauli blocking of the nucleon in the intermediate state of the nucleon pole contribution to the self-energy calculated in nuclear matter tends to reduce the size of the pole contribution to the self-energy. Since the imaginary part of this contribution to the self-energy corresponds to the absorption of the pion on a nucleon, neglect of Pauli blocking in this contribution will tend to overestimate the role of absorption in the self-consistent $t$ matrix. Unlike the cut contribution, introduction of the many-nucleon degrees of freedom does not significantly modify the nucleon pole contribution to the self-consistent $t$ matrix. Therefore, for a first approximation to the nucleon pole contribution to the self-energy, we use a form calculated using the free $t$ matrix with the momentum of the intermediate state nucleon constrained to be larger than the Fermi momentum,

$$\Sigma_P^{RP}(k,\omega)=\frac{g_\pi^2\phi^2(k)k^2}{2m^2\omega_k}\int\frac{d^3p}{(2\pi)^3}\,\frac{\theta(k_F-|\vec{p}\,|)\theta(|\vec{k}+\vec{p}\,|-k_F)}{\varpi+\frac{p^2}{2m}-\frac{(\vec{k}+\vec{p})^2)}{2m}+i\eta}$$

$$=\frac{g_\pi^2\phi^2(k)k}{16m^2m\omega_k}\left[-i\pi\left\{2m\varpi\theta(2k_F-k)\theta\left[\frac{kk_F}{m}-\frac{k^2}{2m}-\varpi\right]\theta(\varpi)\right.\right.$$

$$+\left[k_F^2-\frac{m^2}{k^2}\Omega_N^2\right]\left[\theta(k-2k_F)\theta\left[\frac{kk_F}{m}+\frac{k^2}{2m}-\varpi\right]\theta\left[\varpi-\frac{k^2}{2m}+\frac{kk_F}{m}\right]\right.$$

$$\left.\left.\left.+\;\theta(2k_F-k)\theta\left[\frac{kk_F}{m}+\frac{k^2}{2m}-\varpi\right]\theta\left[\varpi-\frac{kk_F}{m}+\frac{k^2}{2m}\right]\right]\right\}+\theta(2k_F-k)$$

$$\times\left[2m\bar\omega\ln\left|\frac{\bar\omega}{\Omega_{\rm N}+\frac{k^2}{m}-\frac{kk_F}{m}}\right|+\left[k_F^2-\frac{m^2}{k^2}\Omega_{\rm N}^2\right]\ln\left|\frac{\Omega_{\rm N}+\frac{k^2}{m}-\frac{kk_F}{m}}{\Omega_{\rm N}-\frac{kk_F}{m}}\right|+m\Omega_{\rm N}+\frac{k^2}{2}kk_F\right]$$

$$+\,\theta(k-2k_F)\left[\left[k_F^2-\frac{m^2}{k^2}\Omega_{\rm N}^2\right]\ln\left|\frac{\Omega_{\rm N}+kk_F}{\Omega_{\rm N}-\frac{kk_F}{m}}\right|+\frac{2mk_F}{k}\Omega_{\rm N}\right]\Bigg]\,, \tag{46}$$

where $\bar\omega=\omega-B$ and $\Omega_{\rm N}=\bar\omega-(k^2/2m)$. The cut contribution is calculated directly from the free $t$ matrix and is given by

$$\Sigma^{0RC}(k,\omega)=-\frac{\phi^2(k)m_\Delta}{12\pi^2k\omega_k}\Bigg\{\int_{\Omega_\Delta+(\delta k_F^2/2m)-(kk_F/m_\Delta)}^{\Omega_\Delta+(\delta k_F^2/2m)+(kk_F/m_\Delta)}d\mathscr{E}\,H^{0RC}(\mathscr{E})\left[\frac{m^2k^2}{m_\Delta^2}+2(\mathscr{E}-m_\Delta)m\delta\right]$$
$$\times\left[k_F^2-\left[\frac{mk}{m_\Delta\delta}-\{[(2m/\delta)(\mathscr{E}-\Omega_\Delta)]+[(m^2k^2)/(m_\Delta^2\delta^2)]\}^{1/2}\right]^2\right]$$
$$+\theta\left[\frac{m_\Delta\delta k_F}{m}-k\right]\int_{\Omega_\Delta-(mk^2/2\delta m_\Delta)}^{\Omega_\Delta+(\delta k_F^2/2m)+(kk_F/m_\Delta)}d\mathscr{E}\,H^{0RC}(\mathscr{E})$$
$$\times\left[\frac{m^2k^2}{m_\Delta^2}+2(\mathscr{E}-m_\Delta)m\delta\right]$$
$$\times\frac{4mk}{m_\Delta\delta}\{[(2m/\delta)(\mathscr{E}-\Omega_\Delta)]$$
$$+[(m^2k^2)/(m_\Delta^2\delta^2)]\}^{1/2}\Bigg\}\,, \tag{47}$$

where $\Omega_\Delta=\bar\omega-(k^2/2m_\Delta)$ and

$$H^{0RC}=\sum_I(I+1/2)H_{2I}^{0RC}\,.$$

The sum of (46) and (47) is then used as an approximation to the self-consistent self-energy in (42) to calculate $F(\epsilon,L)$. The calculation of $F(\epsilon,L)$ still poses some problems from a computational standpoint. Two levels of integration are displayed explicitly in (42) while the cut contribution contains another explicit integration plus the dispersion integrals (17) needed to calculate $H_{2I}^{0RC}$ giving a total of four levels of integration. Further complication arises from the analytic structure of the dressed propagator in (42). This propagator has branch cuts corresponding to the cuts in the pole and cut contributions to $\Sigma$ plus a simple pole corresponding to a renormalization of the free pion propagation pole. The positions of these singularities in the complex $\Sigma$ plane is dependent on the value of the loop momentum $q$ which complicates the selection of quadrature points for evaluating (42). The calculation can be made much more tractable by approximating the self-energy $\Sigma$ given by (44) and (47) by a sum of complex simple poles

$$\Sigma(q,\mathscr{E})\cong\sum_{i=1}^{3}\frac{a_i(q)}{\mathscr{E}-b_i(q)}\,, \tag{48}$$

where $a_i(q)$ and $b_i(q)$ are complex functions of $q$. Since the cut contribution to $\Sigma$ is dominated by the $P33$ resonance, it is no surprise that it can be well represented numerically by fitting it to a single complex pole. The main defect of such an approximation is that the sharp thresholds of the imaginary part of $\Sigma^{RC}$ are replaced by a function which has an imaginary part everywhere. Since this approximation is used only inside a loop integral where it is averaged over many values of the momentum $q$, it should have no appreciable effect on the qualitative feature of the self-consistent amplitudes. The sum of two complex pole terms is used to approximate the pole contribution to $\Sigma$ in order to minimize the contribution of the imaginary tail of the fitted form below the sharp threshold exhibited by (46). Since it is difficult to fit such a form to (46) for $q<2k_F$ where the Pauli blocking effects become important, the form used for $q>2k_F$ is simply continued to the lower values of $q$. Pauli blocking is included by multiplying the pole contribution by an additional function of $q$, which makes the integrated area of the imaginary part of $\Sigma_p^p$ for each value of $q$ the same for the fitted function and the expression given by (46). Since the imaginary part of $\Sigma_p^p$ corresponds to the strength of absorption, this approximation will maintain the same overall absorption strength as the "exact" $\Sigma_p^p$ given by (46) although it will be distributed somewhat differently. Again, because of the sum over the loop moment, this should be a good approximation. It should also be mentioned that the absolutely sharp thresholds in the self-energy in (46) and (47) are artifacts of the sharp theta-function momentum distribution of the Fermi gas and would not appear in any nuclear model with a more realistic momentum distribution.

Once the self-energy is approximated by a sum of three complex poles as in (48), it becomes clear that the dressed propagator can be written as the sum of four complex poles by rationalizing the propagator and rewriting it as a sum of partial fractions

$$\frac{1}{\mathscr{E}-\omega_q-\Sigma(q,\mathscr{E})+i\eta}\cong\sum_{i=1}^{4}\frac{A_i(q)}{\mathscr{E}-B_i(q)} . \tag{49}$$

The integral over $\mathscr{E}$ in (42) can then be done analytically. The remaining integral over $q$ can now be done easily since the integrand contains only logarithmic singularities which can be located easily.

The right-hand cut contribution to the self-consistent self-energy can then be found from the self-consistent amplitude $H^{RC}$ and is given by

$$\Sigma^{RC}(k,\omega)=-\frac{\phi^2(k)}{6\pi^2\omega_k k}\int_0^{k_F}dp\,p\int_{|p-k|}^{p+k}dL\,L\,[(1-\delta)k^2-\delta(1-\delta)L^2+\delta^2p^2]H^{RC}\left[\omega-B+m+\frac{p^2}{2m}-\frac{L^2}{2m_\Delta},L\right] . \tag{50}$$

The self-energy is related to the Klein-Gordon optical potential $\prod(k,\omega)$ (the invariant self-energy) by the relation

$$\prod(k,\omega)=2\omega_k\sum(k,\omega) . \tag{51}$$

### B. Results for the nuclear matter case

The nuclear matter calculation described in the previous subsection depends on three adjustable parameters, the Fermi momentum $k_F$, and the binding energy $B$, which describe the average properties of the nuclear matter, and a form factor mass $\mu$, which is used to parametrize the half-off-mass-shell $\pi$N amplitudes in terms of the on-mass-shell forward scattering amplitudes according to (6). For the calculations presented here, these parameters are chosen to have the values $k_F=1.9m_\pi c$, $B=0.4m_\pi c^2$, and $\mu=6.7227m_\pi c^2$ (the nucleon mass). For convenience the phase shifts used in (7) are taken from a simple parametrization.[15]

In Ref. 1, it was shown that the self-energy calculated using a static $\pi$N $t$ matrix can be written in the form

$$\Sigma(k,\omega)=-\frac{k^2}{2\omega_k}\phi^2(k)W(\omega) . \tag{52}$$

The separability of this self-energy is a consequence of the use of a static approximation to the free $t$ matrix. The momentum dependence of this self-energy is contained entirely in the off-shell $\pi$n form factor and a kinematical factor which reflects the use of only $P$-wave contributions to the $t$ matrix in calculating $\Sigma$. In order to display the additional momentum dependence of the nonstatic and self-consistent self-energies, the dimensionless quantity, which for convenience will be referred to as the dimensionless self-energy

$$W(k,\omega)=-\frac{2\omega_k\Sigma(k,\omega)}{k^2\phi^2(k)} , \tag{53}$$

is plotted in Figs. 11–14 as a function of the total pion energy $\omega$ for fixed momentum values of $0.5m_\pi c$, $1.0m_\pi c$, and $3m_\pi c$, respectively. The real and imaginary parts of $W(k,\omega)$ resulting from three different calculations of $\Sigma$ are plotted in each figure. Curve 1 represents $W(k,\omega)$ calculated using the static approximation to the free $t$ matrix and serves as a reference for studying the momentum dependence of the other two calculations since it is independent of $k$. Curve 2 is $W(k,\omega)$, calculated using the nonstatic free $t$ matrix given by (18), and curve 3 is $W(k,\omega)$, calculated using the self-consistent amplitudes

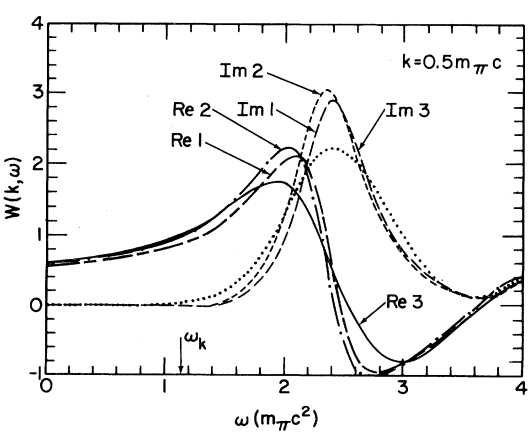


FIG. 11. Dimensionless self-energy calculated using static (curve 1), nonstatic (curve 2), and self-consistent $t$ matrices as a function of pion energy $\omega$ at fixed pion momentum $k=0.5m_\pi c$.

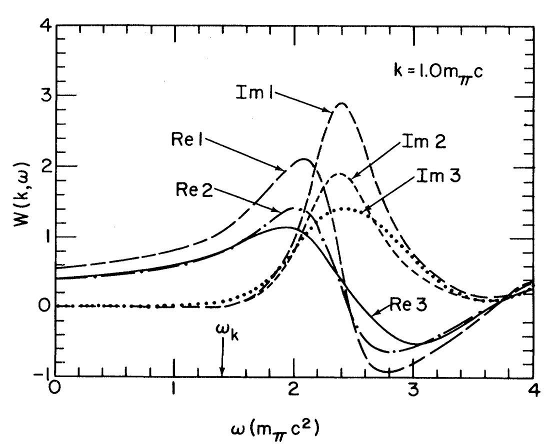


FIG. 12. As in Fig. 11, but with $k=1.0m_\pi c$.

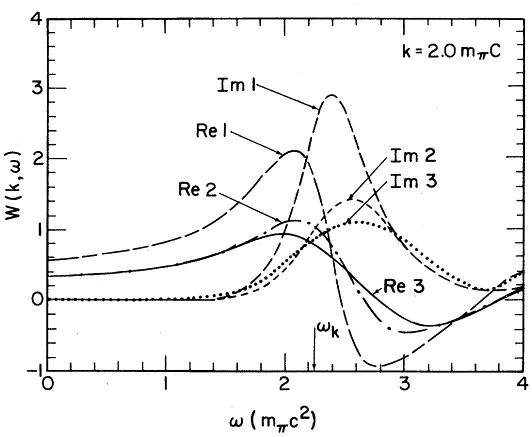


FIG. 13. As in Fig. 11, but with $k=2.0m_\pi c$.

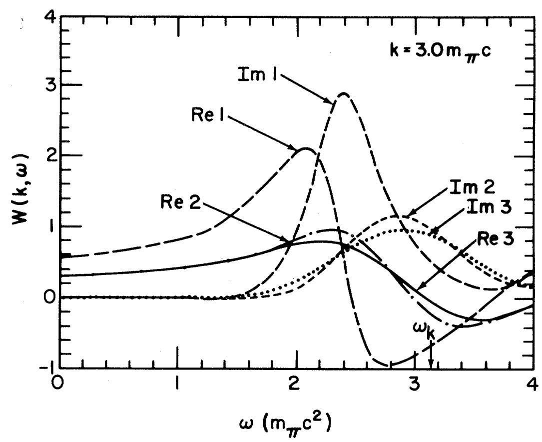


FIG. 14. As in Fig. 11, but with $k=3.0m_\pi c$.

defined by (43). In order to simplify the discussion below, the calculations represented by curves 1, 2, and 3 will be referred to as static, nonstatic, and self-consistent, respectively. In each of these four figures, an arrow marks the energy of an on-shell pion having the same momentum as is used in that figure.

Comparison of the nonstatic calculations (curve 2) to the static calculation (curve 1) in Figs. 11—14 shows the additional momentum dependence of the self-energy associated with the kinematical transformation of the free $t$ matrix from the $\pi$N c.m. frame to the nuclear rest frame. As the momentum $k$ increases, the peak in the imaginary part of the self-energy is moved to higher energy $\omega$ and the breadth of the peak is increased relative to the static self-energy. This is primarily due to the recoil energy of the intermediate state of the nonstatic $t$ matrix and the Fermi average of nucleon momenta. Notice also the rapid decrease in magnitude of the peak in the imaginary part of the nonstatic self-energy relative to the corresponding peak in the static self-energy in going from $k=0.5m_\pi c$ to $k=1m_\pi c$. This is a result of the form of the pion c.m. momenta defined by (16) which appear in the $P$-wave projection operators (15a). Since the pion c.m. momentum depends on the total $\pi$N pair momentum $L$, it no longer goes to zero as the laboratory pion momentum $k$ goes to zero when the nucleon momentum is nonzero. As a result, while the static self-energy $\Sigma$ goes to zero as $k^2$ the nonstatic self-energy is finite at $k=0$ due to the Fermi averaging. The dimensionless self-energy $W$ for the nonstatic calculation is therefore going as $1/k^2$ as $k$ approaches zero while the static $W$ remains constant. These contributions to the nonstatic self-energy which are finite at $k=0$ would appear as $S$-wave contributions to the pion optical potential in a finite nucleus calculation.

Comparison of the self-consistent calculation (curve 3) to the nonstatic calculation (curve 1) shows the result of introducing nuclear many-body degrees of freedom into the intermediate states of the effective $\pi$N $t$ matrix in the nuclear medium. This introduces a dynamical broadening of the resonance in addition to the kinematical broadening of the nonstatic calculation. Notice that the imaginary part of the self-consistent self-energy persists below the threshold of the imaginary part of the nonstatic self-energies. This is a direct signature of the absorption of pions on two or more nucleons in intermediate states of the effective $t$ matrix. The full width at half maximum and the peak position for each of the calculations in Figs. 11—14 is summarized in Table I.

The momentum dependence of the self-consistent self-energy is summarized in Fig. 15. This figure shows the imaginary part of the dimensionless self-energy corresponding to the curves labeled Im3 in Figs. 11—14. In Fig. 15, each of these curves is represented by a solid line and labeled with the value of the pion momentum. The shifting, spreading, and change in magnitude with increasing pion momentum is clearly illustrated.

The dashed curve in Fig. 15 represents the imaginary part of the static, self-consistent dimensionless self-energy. This is calculated as in Ref. 1, but with the parameters specified at the beginning of this section. It is clear that the momentum dependence of the nonstatic calculation makes it impossible for the static self-consistent calculation to provide a reasonable representation of the self-energy over the range of momentum values. It should

TABLE I. Widths and positions of resonant contributions to the imaginary part of the dimensionless self-energy for static, nonstatic, and self-consistent calculations at $k=0.5$, 1.0, 2.0, and $3.0m_\pi c$.

| | FWHM ($m_\pi c^2$) | | | Peak position ($m_\pi c^2$) | | |
|---|---|---|---|---|---|---|
| $k$ ($m_\pi c$) | Static | Nonstatic | Self-consistent | Static | Nonstatic | Self-consistent |
| 0.5 | 0.669 | 0.687 | 1.012 | 2.394 | 2.340 | 2.386 |
| 1.0 | 0.669 | 0.731 | 1.050 | 2.394 | 2.374 | 2.410 |
| 2.0 | 0.669 | 0.891 | 1.198 | 2.394 | 2.553 | 2.611 |
| 3.0 | 0.669 | 1.100 | 1.336 | 2.394 | 2.853 | 2.904 |

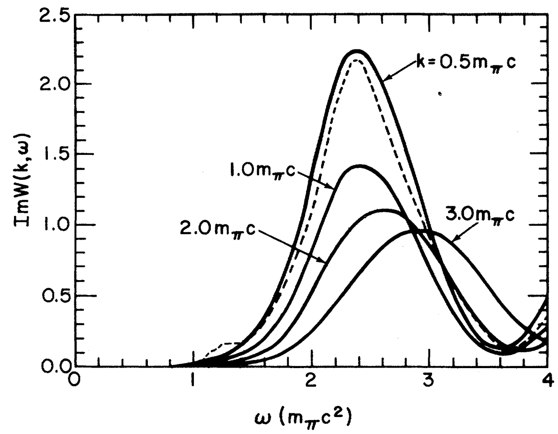


FIG. 15. Summary of the imaginary parts of the self-consistent, dimensionless self-energy (curve 3) from Figs. 11—14 (solid lines). The dashed line is the imaginary part of the static, self-consistent, dimensionless self-energy calculated as in Ref. 1.

also be noted that the large value of the imaginary part of the static self-consistent self-energy in the region of the pion threshold energy shows that the static calculation overemphasizes the importance of many-nucleon pion absorption intermediate states.

Figure 16 shows the negative of the self-energy $\Sigma$ for on-shell pion momenta as a function of pion energy for each of the three calculations as presented in Figs. 11—14. The arrows indicate the on-shell energies for each of the momentum values represented in Figs. 11—14. It is clear that the nonstatic and self-consistent self-energies differ considerably from the static self-energy. The self-consistent self-energy is broadened substantially relative to the nonstatic self-energy. Notice also that the real parts of the nonstatic and self-consistent self-energies are nonzero at $\omega = 1m_\pi c^2$, which corresponds to $k = 0m_\pi c$ as was argued above.

As was shown above, the medium modifications to the $P11$ pole contribution to the effective $t$ matrix can be described in terms of a vertex modification and an optical potential for the intermediate state nucleon. From (45) it can be seen that the vertex modification is given by

$$f_{\pi\text{N}} = \frac{1}{1 + H_1^{0RC}\left[\epsilon - \dfrac{L^2}{2m_\Delta}\right] F(\epsilon, L)} f^0_{\pi\text{N}} \tag{54}$$

for each absorption or emission vertex, while the nucleon optical potential is given by

$$V_\text{N}(\epsilon, L) = -\frac{3g_\pi^2}{4m^2}\left[\frac{F(\epsilon, L)}{1 + H_1^{0RC}\left[\epsilon - \dfrac{L^2}{2m_\Delta}\right] F(\epsilon, L)}\right]. \tag{55}$$

Figure 17 shows the ratio of the modified vertex to the free vertex, $f_{\pi\text{N}}/f^0_{\pi\text{N}}$. Since the contribution of this term comes primarily from the neighborhood of the nucleon pole, and since the position of the pole is expected to differ little from that of the free nucleon pole, the energy at which the ratio of vertex functions is evaluated in this figure is the energy of the free pole. The curves are displayed as a function of $L$ which is the momentum of the intermediate state nucleon. It is clear that the real part of this ratio differs from 1 by only a small amount, while the imaginary part of the ratio remains close to zero. Therefore, the vertex renormalization of the pole is only a small effect.

Figure 18 shows the nucleon optical potential (55) at the energy of the free nucleon pole as a function of the nucleon momentum $L$. As was mentioned above, this optical potential consists of a rather peculiar subset of contributions to the complete nucleon optical potential which include only contributions containing the exchange of two pions. One-meson exchange pieces and heavy-meson exchanges are not included. It is clear that the optical potential as shown in this figure bears little resemblance to phenomenological optical potentials and is shown here only for the sake of completeness of this discussion. If an optical potential is to be used for nucleons above the Fermi sea, a more realistic form of the optical potential should be used in place of (55).

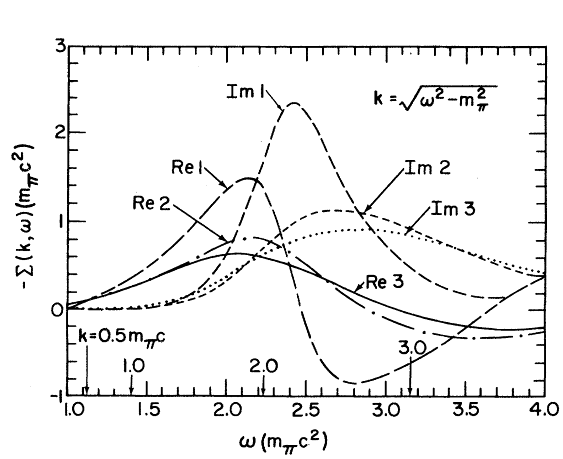


FIG. 16. The negative of the self-energy as a function of pion energy with pion momentum determined by the mass-shell condition. The three sets of curves are labeled as in Fig. 11.

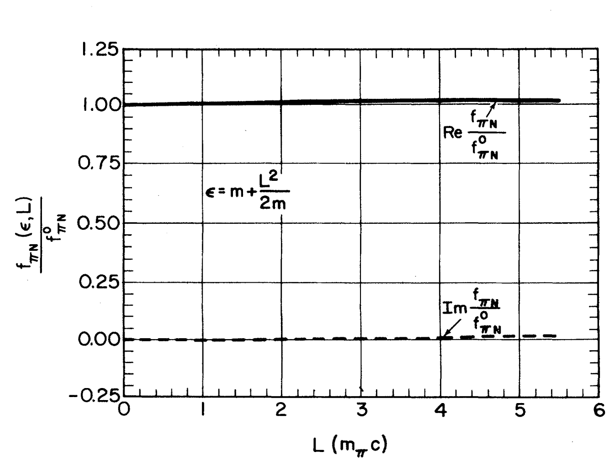


FIG. 17. The ratio of the medium modified vertex function to the free vertex function as a function of the nucleon momentum $L$.

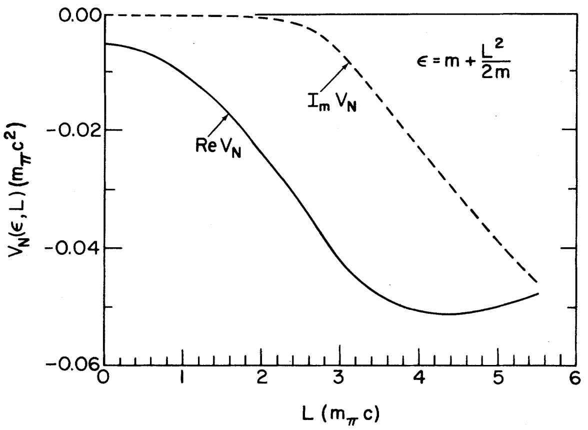


FIG. 18. Contributions to the nucleon optical potential corresponding to (55) as a function of nucleon momentum $L$.

## IV. DISCUSSION AND CONCLUSIONS

It is clear from the results shown above that the calculation of the nonstatic, self-consistent $\pi$N $t$ matrix in nuclear matter has all of the qualitative features which would be expected from physical considerations. That is, the resonance is broadened and shifted by the introduction of additional intermediate reaction channels, and the presence of many-nucleon absorption channels lowers the threshold of the imaginary part of the self-consistent optical potential relative to that of the first-order optical potential. Some caution, however, should be used in attempting to extract quantitative information from such calculations due to certain complications which arise from the properties of nuclear matter.

To understand the origin of one of these complications, it is useful to consider the self-consistent $t$ matrix calculation for a finite nucleus. The self-consistent $t$ matrix is constructed so as to sum a set of contributions to pion-nucleus scattering where the pion scatters from a nucleon, is scattered from the nuclear core, and then scatters again from the valence nucleon. The self-consistent $t$-matrix sums contributions which involve any number of reflections of the pion between the valence nucleon and the core, where the initial and final scattering always occur on the valence nucleon. In a finite nucleus where the nuclear wave functions are localized, these multiple reflections can only occur if the pion is always reflected back into the region where the nuclear wave functions are non-negligible. This back scattering requires that momentum is transferred between the pion and the nucleons and that the magnitude of the momentum which can occur in the internal loop of the self-consistent $t$ matrix is regulated by the nuclear momentum distribution. In nuclear matter, the nuclear wave functions are infinite plane waves, and elastic scattering of the pion from the nuclear medium is always in the forward direction. Therefore, the pion and nucleon can continue to scatter without transferring momentum to the medium, with the result that nuclear momentum distribution does not regulate the magnitude of the loop momentum in the self-consistent equation. This momentum is then only regulated by the $\pi$N off-shell form factors and the results of the calculation will be sensitive to the functional form of the form factor and the form factor mass. For the purpose of the calculation presented in this paper, a Gaussian form factor (38) with a form factor mass equal to the nucleon mass was chosen to avoid any problems which might arise from the use of nonrelativistic kinematics.

The second complication has to do with the reactive content of the effective $t$ matrix. From unitarity considerations and the form of the self-consistent $t$-matrix equation, it is possible to relate the imaginary part of the self-consistent self-energy to a sum of exclusive reaction cross sections characterized by the number and type of particles in the final state, such as 1p-1h, 1p-1h-1$\pi$, 2p-2h, 2p-2h-1$\pi$, etc. The expression for the reactive content of the optical potential can then be used to test the calculated optical potential for consistency with measurement of the total absorption cross section, for example. Since nuclear matter is infinite in extent and capable of absorbing pions, any pion which is placed in nuclear matter will eventually be absorbed. Nuclear matter, therefore, has a reactive content which consists completely of absorption channels such as 1p-1h, 2p-2h, 3p-3h, etc. Indeed, a careful examination of the reactive content of the self-consistent $t$ matrix in nuclear matter shows this to be rigorously true. Since the total reaction cross section for $\pi$-nucleus scattering is not composed entirely of absorption, this is a very unsatisfactory situation. This problem is due entirely to the fact that all elastic scatterings from nuclear matter are in the forward direction. Naive approaches to a local density approximation of the self-consistent $t$ matrix for finite nuclei will also have this problem with reactive content. A believable comparison of the effects of the self-consistent $t$-matrix approach to $\pi$-nucleus scattering with data will require an actual solution of the self-consistent $t$-matrix equations in a finite nucleus.

The conclusions which can be drawn from the calculation presented in this paper can be summarized as follows.

(1) The resonant contribution to the self-consistent pion self-energy is 20% to 50% greater in width than the first-order, nonstatic self-energy. The effective mass of the self-consistent resonance is about 10 MeV greater than the free resonant mass.

(2) The modification of the pion absorption and emission vertex resulting from the calculation of the self-consistent $\pi$N $t$ matrix is negligible.

(3) The part of the self-consistent $\pi$N $t$ matrix which has the form of a nucleon optical potential can be isolated and replaced by a better representation of the nucleon optical potential. This eliminates any double counting which may occur in the calculation of the self-consistent $t$ matrix.

## ACKNOWLEDGMENTS

The author would like to thank M. K. Banerjee and S. J. Wallace for the many discussions of this problem which he has had with them. The support of the U.S. Department of Energy and the University of Maryland Computer Science Center for this research is gratefully acknowledged.

[1]J. W. Van Orden, M. K. Banerjee, D. M. Schneider, and S. J. Wallace, Phys. Rev. C **23**, 2157 (1981).

[2]R. M. Frank, J. L. Gammel, and K. M. Watson, Phys. Rev. **102**, 891 (1956).

[3]L. S. Celenza, L. C. Liu, W. Nutt, and C. M. Shakin, Phys. Rev. C **14**, 1090 (1976).

[4]M. B. Johnson and H. A. Bethe, Nucl. Phys. **A305**, 418 (1978); M. B. Johnson and B. D. Keister, *ibid.* **A305**, 461 (1978).

[5]C. Schmit, Nucl. Phys. **A360**, 359 (1981).

[6]R. Cenni and G. Dillon, Nucl. Phys. **A392**, 438 (1983).

[7]E. Oset and W. Weise, Nucl. Phys. **A319**, 477 (1979).

[8]D. M. Schneider, M. K. Banerjee, J. W. Van Orden, and S. J. Wallace, Phys. Rev. C **25**, 979 (1982).

[9]C. Schmit, Nucl. Phys. **A192**, 449 (1972).

[10]J. P. Maillet, J. P. Dedonder, and C. Schmit, Nucl. Phys. **A271**, 253 (1976).

[11]M. Hirata, F. Lenz, and K. Yasaki, Ann. Phys. (N.Y.) **108**, 116 (1977).

[12]R. S. Bhalerao, L. C. Liu, and C. M. Shakin, Phys. Rev. C **21**, 2103 (1980).

[13]M. K. Banerjee and J. B. Cammarata, Phys. Rev. C **17**, 1125 (1978). It is also possible to obtain the amplitudes by a direct solution of the nonlinear integral equations resulting from the truncated Low expansion. A nonstatic solution of this equation is presented in the above paper and in: M. K. Banerjee and J. B. Cammarata, Phys. Rev. D **16**, 1334 (1977); Nien-Chih Wei and M. K. Banerjee, Phys. Rev. C **22**, 2052 (1980); **22**, 2061 (1980). These calculations give *S*- and *P*-wave phase shifts which are in good agreement with experiment. In the last of these references it is shown that the method used in this paper and the direct solution method give consistent results provided that a sufficiently large form factor mass is used.

[14]M. K. Banerjee and G. E. Walker, Phys. Rev. C **27**, 657 (1983).

[15]M. Salomon, TRIUMF report, TR1-74-2, 1974.